ORIGINAL PAPER

Experimental evaluation of alternative ceiling-based ventilation systems for long-range passenger aircraft

Tobias Dehne[1] · Pascal Lange[1] · Daniel Schmeling[1] · Ingo Gores[2]

Abstract

Alternative ventilation technology bricks, such as ceiling-based, sidewall-based or floor-based ventilation, are of high interest in terms of manufacturing and customization benefits for passenger aircraft. Two novel ventilation systems and state-of-the-art Mixing Ventilation (MV) were experimentally investigated under static conditions in a ground-based research facility. In case of Micro-Jet Ventilation, a perforated ceiling brings the air into the cabin as localized micro-jets with high momentum. Further, Low-Momentum Ceiling Ventilation characterized by a low-momentum air supply through planar and large-surface inlets is investigated. The measurement techniques and the test matrix were designed in order to quantify and evaluate thermal comfort, local air quality and energy efficiency of the ventilation concept. The results proved that there is not one single ventilation concept which optimizes all challenges: air quality, thermal comfort and energy efficiency. Both advantages and disadvantages were found for each ventilation system. In terms of technology bricks, the following main results were found: The average local age-of-air was between 5 and 14%, depending on the boundary conditions. It was lower for the ceiling-based concepts compared to state-of-the-art MV. At the same time the average CO_2 concentration decreased by 7–14% for the ceiling-based concepts compared to MV. The local velocities in the vicinity of the passengers were similar for cruise conditions, whereas they decreased by up to 38% in case of hot-day-on-ground conditions for ceiling-based ventilation compared to MV. On the other hand, the heat removal efficiency was low for all concepts and the temperature stratification increased in case of ceiling-based ventilation.

Keywords Aircraft cabin mock-up · Realistic thermodynamic boundary conditions · Novel ventilation concept · Thermal passenger comfort · Air quality · Energy efficiency

1 Introduction

Novel ventilation systems for aircraft cabins have attracted the attention of scientists and aircraft manufacturers during the last years due to their potential of energy saving and in terms of providing a higher level of thermal comfort. Technological innovation at all levels of aircraft design is the key to reduce the CO_2 emissions generated by the global fleet by 50% by 2050, for more information see [1]. Furthermore, the Environmental Control System (ECS) requires up

to 75% of the non-propulsive power to ventilate a passenger aircraft under normal flight conditions "Cruise" [2]. With a general trend of increasing heat loads in modern passenger cabins, the interest of the aircraft industry in novel ventilation systems is gaining more and more importance. Further challenges are: improved thermal passenger comfort, a higher level of air quality and the possibility to adapt the cabin layout to different requirements. Therefore, previous studies comprise numerical and experimental investigations of alternative ventilation systems in single-aisle as well as in twin-aisle aircraft cabins [3–6]. For cabin displacement ventilation in specific, this results in high heat removal and low draft rates; for more details see [7]. To evaluate novel ventilation concepts under realistic stationary and non-stationary boundary conditions, flight tests were conducted in an A320 of the German Aerospace Center (DLR) and analyzed in [8, 9]. During these pioneering, but also very expensive measurement flights, different thermodynamic

✉ Tobias Dehne
  tobias.dehne@dlr.de

1 German Aerospace Center (DLR), Institute of Aerodynamics and Flow Technology, Bunsenstraße 10, 37073 Göttingen, Germany

2 Airbus Operations GmbH, Kreetslag 10, 21129 Hamburg, Germany

boundary conditions (e.g., temperatures of the cabin interior surfaces) depending on the flight and operational phases were recorded. Flight testing is quite costly and time-consuming due to the detailed and lengthy planning, including the flight certification requirements. Furthermore, the applicable measurement systems within an aircraft cabin during a flight scenario are limited and the test scenario is restricted to existing and available aircraft geometries. Therefore, experimental investigations of the cabin air environment are normally carried out on special test benches at ground level, with many studies focusing on cabin layouts characterized by single-aisle configurations [7, 10]. Selected two-aisle arrangements, e.g., a 767–300 cabin model have also been studied experimentally [5, 11]. However, very simplified environments (i.e., very short cabin sections) have been used in contrast to real aircraft cabins, thus limiting the transferability of the results to realistic operational aircraft scenarios. In addition, there are no published studies to date addressing the performance of alternative ventilation systems for long-range commercial aircraft under transient or non-ideal boundary conditions.

In order to avoid the complex and very expensive measurement flights, a new full-size cabin mock-up for long-range aircraft was developed for testing alternative air distribution systems under static and dynamic boundary conditions [12]. The mock-up offers the possibility to simulate different flight phases in operationally relevant temperature and time scales under stationary and dynamic conditions with well-defined thermal boundary conditions. A comparison of a data set from real flight tests with a fully simulated flight in the new mock-up highlights the feasibility of experimentally simulating different flight phases on ground [12]. The main focus of the study is put on the two operating modes "Cruise" and "Waiting for departure" (Hot day on ground "HDoG"), with thermal passenger comfort and efficiency being investigated experimentally [13]. The aim of this study is to compare two novel ventilation options with state-of-the-art MV in the new full-scale, long-range aircraft cabin mock-up under static "Cruise" and "HDoG" conditions. Both advantages and disadvantages were found for each ventilation system. The present work is of great importance to improve the ventilation systems of future aircraft.

2 Experimental set-up

2.1 Modular cabin mock-up

The new modular cabin mock-up (in German: "Modulares Kabinen Mock-Up Göttingen"-MKG) [12] of the German Aerospace Center (DLR) in Göttingen was developed, set up and chosen as a test platform for the presented studies. It is a test bed for aircraft cabin research activities at ground level

representing a full-size (1:1 scale) cabin section of modern wide-body airliners in the current expansion stage. The inner dimensions comprise a total length of $L = 9.96$ m, a width of $W = 6.25$ m and a height of $H = 2.7$ m. For the investigation of novel aircraft ventilation systems, it is crucial that the experiments provide geometric similarity to real aircraft cabins. Therefore, the entire interior panels (e.g., sidewalls, lateral and center overhead bins, ceiling panels as well as dado panels) consist of original, second-hand aircraft parts. Further, the seats are also original aircraft seats to ensure a realistic seating arrangement. A twin-aisle cabin layout is realized, characterized by a 10-abreast seating configuration arranged in a 3-4-3 seating layout. During the studies, only economy seating class is implemented. However, the installation of different seating classes, i.e., business, first or economy plus is also possible. The baseline layout provides 10 seat rows with a 32" seat pitch. Hence, the cabin offers space for 100 passengers in total.

Typical flight scenarios (e.g., hot day on ground, climb, cruise) are of great importance when it comes to evaluating new ventilation concepts. It is known from earlier flight tests in the Airbus A320-232 DLR-ATRA [9] that the air temperature in the gap between the primary and secondary insulation of a typical aircraft fuselage ranges from 10 to 35 °C depending on the flight phase (e.g., "Cruise" flight or "HDoG"). Since the surface temperature distribution inside the cabin depends on the different flight phases, the new ventilation approaches must be considered in the evaluation with regard to energy efficiency, passenger comfort and air quality. Based on these findings, the gap temperature was experimentally simulated in this study. Capillary tubes have been attached to the aluminum sheets on the hull elements, and a temperature-controlled water–glycol mixture allows the gap temperature to be precisely set and changed. Closely spaced capillaries in combination with the aluminum sheets ensure a homogeneous temperature distribution on all built-in interior parts (Dado, side wall and ceiling panels, roof compartments, floor). The front and back of the cabin model are not actively temperature-controlled since we only investigate a segment of the cabin and thus simplified adiabatic boundary conditions can be assumed here. These are realized by thermally insulated walls and outside temperatures around the mock-up similar to the mean cabin temperature. For more details, see [12].

2.2 Ventilation systems

To compare the results of two novel ventilation systems with a reference case for a long-range aircraft, a generic version of MV—which is state-of-the-art for ventilation of passenger aircraft—was investigated in the modular cabin mock-up. Figure 1 shows the basic principles of the examined ventilation systems:
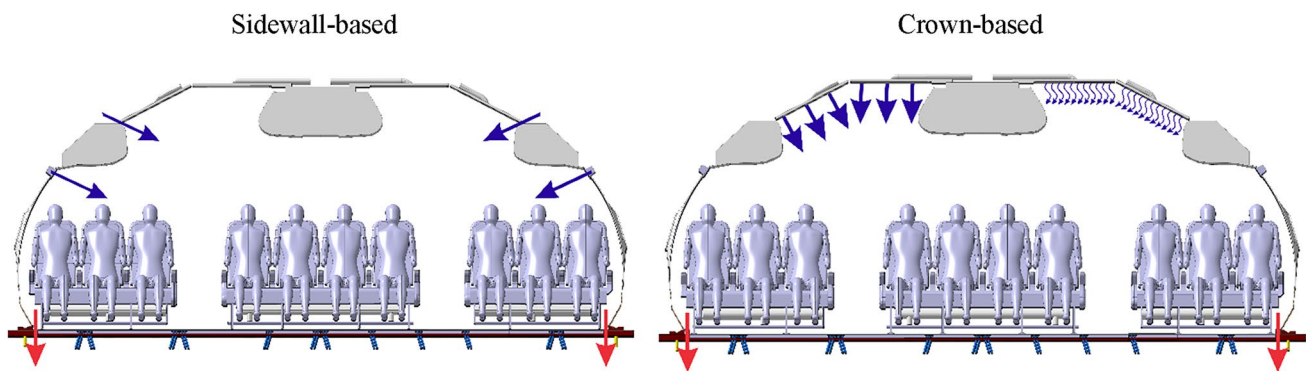
Sidewall-based   Crown-based

Fig. 1 Cabin cross-sectional view for MV (left) as well as for MJV and LMCV (right) ventilation concepts in the cabin mock-up. The straight arrows in Figure right indicate the faster jets at MJV, the wavy lines show the lower inflow velocities at LMCV. Please note that during measurement either MJV or LMCV was installed at all elements, they are only combined in the figure for the sake of brevity

- <u>Sidewall-based system</u> (Fig. 1, left)

    o Mixing Ventilation (MV) is characterized by a high degree of mixing of jets of fresh air entering the cabin on both sides. It should be noted that in current twin-aisle aircraft, MV systems are sometimes operated with an additional ceiling outlet, which was not installed in our pure sidewall-based MV system.

- Two <u>crown-based ventilation systems</u> (Fig. 1, right) allow for a complete ventilation from the ceiling area

    o Micro-Jet Ventilation (MJV), the state-of-the-art in train air conditioning, characterized by a high degree of mixing of the jets of fresh air entering the cabin in the aisle area [14].

    o Low-Momentum Ceiling Ventilation (LMCV), characterized by a low-momentum air supply through planar and large-surface inlets, which are similarly aligned as MJV in the ceiling area with two slanted and two straight inlets in the cross section.

For optimal ventilation, four MV air inlets were installed in the cross section, two ceiling inlets above and two air inlets below (lateral) the luggage compartment, see Fig. 1(left). With nine inlets in longitudinal direction, overall 36 air inlets were installed in the mock-up. For all investigated ventilation systems, the exhaust air openings were located in the lower part on both sides of the cabin (red arrows) close to the Dado panels. For more details, also on the air ducts leading out of the cabin mock-up, see [12]. A generic version of MJV was investigated in the mock-up as an alternative ventilation concept. A perforated ceiling brings the air into the passenger compartment as localized micro jets with high momentum. The installed MJV consists of holes with a diameter of 3 mm at a lateral spacing of 20 mm in each direction, see Fig. 1(right). LMCV, the second ceiling-based novel concept, is characterized by a low-momentum air supply through planar and large-surface inlets, which are similarly aligned as the MJV inlets in the ceiling area with two slanted and two straight inlets in cross section, see Fig. 1(right). The inlet area is made of fabric membranes ensuring a uniform outflow with low and homogeneous flow velocities, see [7]. As described above, the exhaust air openings are located in the lower part on both sides of the cabin (red arrows) close to the Dado panels.

2.3 Modular cabin mock-up measurement techniques

This section provides an overview of the installed measurement technology used to determine the comfort-relevant quantities as well as the key figures to analyze the energy efficiency of the ventilation approach. In addition to the 100 thermal manikins (TMs), the cabin measurement system basically comprises three sensor racks (SR) and an infrared camera setup to analyze the surfaces temperature distribution at the TMs as well as at the inner lining elements. In total, more than 250 sensors were installed in the cabin.

In order to achieve a realistic heat load and realistic dimensions, thermal manikins with a volume of 0.05 m^3 and a surface of 1.52 m^2 were used to simulate the passengers during the experimental investigations [15]. The TMs consist of a foam core wrapped with a resistance wire which allows for individual heating by an external power supply in a range of 0–150 watts for a constant, sensible heat release. Realistic surface temperatures and buoyancy forces were achieved through a very homogeneous distribution of the heat flow density, slightly increased in the head area. For this study, an automatic control of the heat output depending on the average temperature in the cabin was set. The automatic mode allows for the emission of sensible heat depending on the ambient temperature. The underlying

heat-release-cabin-temperature-curve is based on a European standard [16].

The fluid temperatures were measured close to the TMs at a distance of 5 cm and in the aisle section with the aim to record the comfort-relevant fluid temperatures in the vicinity of the passengers and the crew. To evaluate the temperature stratifications near the TMs, measurement racks (see SR1 in Fig. 2) with resistance temperature detectors (RTDs) at four height levels were constructed to monitor the temperatures in a complete seat row. One additional rack with RTDs at 12 different heights was positioned in the aisle section in row 5 to evaluate the temperature stratification in the aisle, see SR3 in Fig. 2(left). Chest-high RTDs were installed in front of all TMs (see red circles in Fig. 2, left) to determine the temperature homogeneity in the complete cabin section. The flow velocities in the cabin—measured close to the TMs at different height levels (ankle, knee, chest, head)—are important for two reasons: First, the velocity should be low enough to prevent draft. Second, the large-scale flow patterns and the small-scale turbulence structure of the cabin flow govern mixing and heat exchange and, thus, determine macroscopic quantities, such as heat removal efficiency, temperature homogeneity and temperature stratifications. Additionally, the probes mounted in row 6 and indicated as SR2 in Fig. 2(left) can also be used to measure the fluid temperatures. They provide an accuracy of ± 0.02 m/s for the velocity and ± 0.2 K for the temperature. In total, 40 combined velocity and temperature probes were installed within the MKG. Using the measurement racks SR1 and SR2, the spatially resolved temperature distribution in two seat rows can be determined. The probes near the TMs are positioned at a distance of 5 cm from the manikins' surface at ankle, knee, chest and head level, as indicated for the RTDs. With

the help of these probes, the comfort-relevant air velocities and their distribution for different body parts and seat rows can be identified. The velocity and temperature measurement system mounted on SR2 is combined with a humidity as well as an operative temperature probe (cyan and orange hexagon in Fig. 2(left), respectively) to determine the thermal passenger comfort criteria, such as predicted mean vote (PMV) and predicted percentage dissatisfied (PPD).

To record the surface temperatures within the cabin, two infrared (IR) cameras were installed in front of the first seat row. The positions of the cameras and the corresponding field of views are depicted in dark green in Fig. 2(left). The IR cameras provide a resolution of 640×480 px and a sensitivity of 0.08 K. Additional infrared images were taken of the side panels at stationary boundary conditions in order to determine the spatial surface temperature distributions.

Air quality is another important parameter for evaluating ventilation systems. The performance of different systems in relation to this quantity can be evaluated by examining the spatially averaged local mean age of the air (AoA) as well as the local CO_2 concentrations.

The installed CO_2 supply system comprises capillaries at the nasal level of the thermal human models, through which a CO_2 volume flow typical for adult humans (0.275 Nl/min) is continuously supplied. The use of capillaries as "noses" ensures a reproducible, homogeneous volume flow at all seating positions, since the largest pressure drop—compared to others in the CO_2 supply system—occurs in these capillaries mounted in the "noses". In total, 40 CO_2 sensors were used to measure the spatial concentration distribution. The sensors were attached to the "Flight Entertainment System" of the front, middle seat of a seating group (see Fig. 3). Using the decay curves, the air
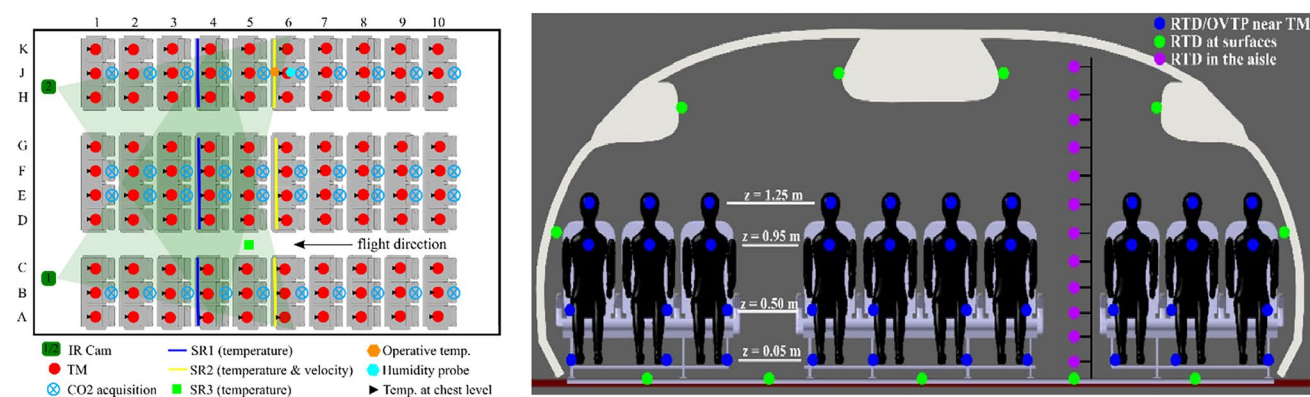

Fig. 2 Cabin layout and measurement installation. Left: top view with thermal manikins (Red circles) including chest temperature probes (Black arrow head). SR1-3 denote the position of the respective sensor racks for temperature SR1 (Blue line), temperature and velocity SR2 (Green square) and aisle temperatures SR3 (Green circle). Further, the position of the comfort measurements, operative temperature (Yellow hexagon) and humidity (Blue hexagon) are indicated. Right: Cross-section view. Position of RTD and OVTP probes near the TMs (blue circles,) mounted at SR1 and SR2 in seat row 4 and 6, respectively. Further, probe position at SR3 (magenta circles,) to capture fluid temperatures in the aisle as well as probes (blue cross circle) for measuring inner surface temperatures and the positions of the CO_2 sensors
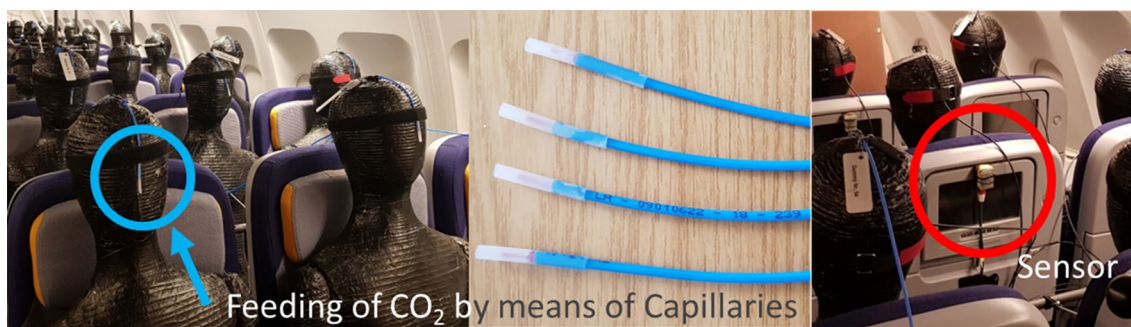
Fig. 3 Measurement setup to determine CO_2 concentrations in an occupied cabin

exchange rate, the local mean air of age and, of course, the concentration values in the saturation state were determined for each sensor position. The measurement positions of all installed CO_2 sensors are illustrated in Fig. 2a.

It should be noted that for the evaluation of the local AoA values the concentration curves at every sensor position were used and a local 'exhalation' of all manikins was supplying the CO_2. Typically, the tracer gas supply is integrated into the central supply air and the decay values in the exhaust of the ventilation system are evaluated. The different approach allows to evaluate the local CO_2 concentrations as an additional evaluation parameter, which is not feasible in case of a central supply and exhaust air concentration measurement.

A representative curve of the local CO_2 concentration during a measurement run is shown in Fig. 4. Starting with the injection of CO_2 at the noses of the TMs, a strong increase up to a constant concentration value can be seen.

After closing the valve, the concentration values decrease depending on the performance of the ventilation system.

3 Investigated cases and evaluation parameters

Using temperature-controlled walls, two different operational phases (characterized in Table 1) were experimentally simulated in the mock-up. The main focus of interest is the "Cruise" case with cold ambient temperatures. Furthermore, the results of the scenario "Hot Day on Ground" ("HDoG"), simulating the warm cabin after a completed boarding procedure with a fully occupied cabin, will be presented in this paper. In both cases, all measurement techniques were used to evaluate the different volume flow distributions of the investigated ventilation systems under static conditions in terms of thermal comfort, heat removal efficiency and (local)

Fig. 4 Progression of CO_2 concentration during a measurement run. The colored bars show the time intervals used to evaluate the different parameters
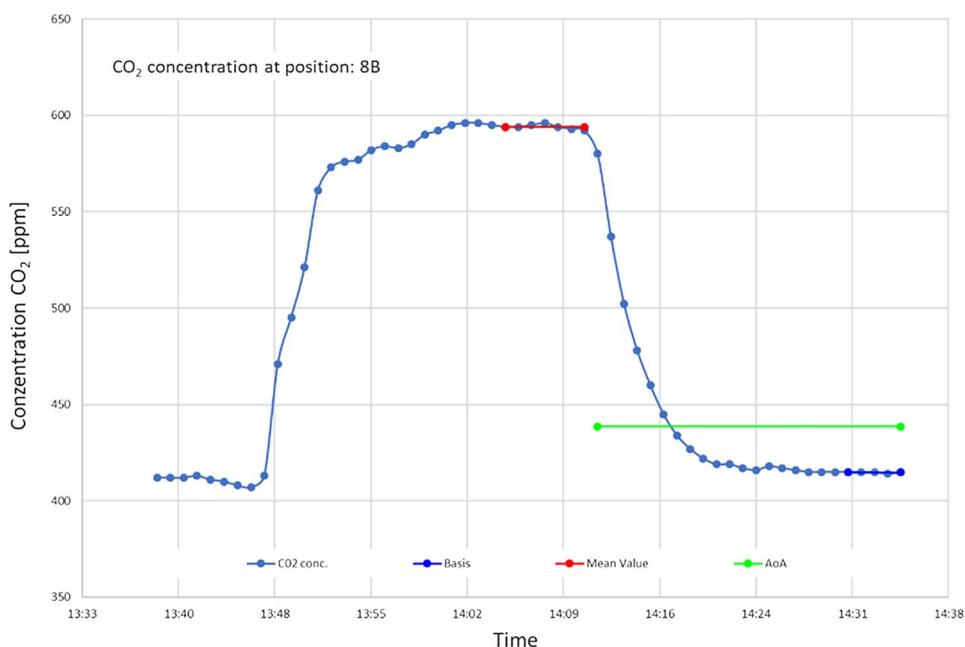
Table 1 Summary of operational phases

	Typical boundary conditions	Main challenges for ventilation system
"Cruise"	• Typical flight condition • Cold temperatures between primary and secondary insulation	• Main operational mode • Efficient operation of complete HVAC system • Long-term comfortable conditions for PAX
Hot day on ground "HDoG"	• Waiting for takeoff, e.g., in Dubai • Very high temperatures between primary and secondary insulation	• Highest cooling demand • Varying thermal loads during boarding • Effective removal of heat • Providing acceptable conditions for PAX

air quality. It should be noted that humidity and ambient pressure were varied in this project.

Table 2 summarizes the parameters and the corresponding measuring positions. To obtain comparable results, a control temperature of $T_{cab} = 23$ °C as mean temperature in the cabin was set for all investigated cases with an ambient temperature of 10 °C for all "Cruise" cases and 35 °C for "HDoG". To reach $T_{cab} = 23$ °C, the supply temperature (T_{in}) was adjusted for the different cases.

The temperatures were evaluated in terms of the temperature differences between head and ankle ($\Delta T_{h\text{-}a}$) as well as between maximum and minimum chest temperatures (ΔT_{chest}). The first value is by definition a parameter for the temperature stratification, which should not exceed certain thresholds. $\Delta T_{h\text{-}a}{}^{seat}$ shows the maximum temperature gradient between head and ankle on any of the 20 seats in row 4 and 6. The temperature variation in the occupied zone (ΔT^{max}) is the difference between the maximum and the minimum temperature in the vicinity of the TMs in the row 3–8. ΔT_{chest} is the difference between the warmest and

the coldest seat in the cabin and is used to determine the spatial temperature homogeneity. Since boundary effects of the front and rear wall occurred in rows 1,2 and 9,10, which cannot be simulated comparable to a real aircraft, these rows were not considered during further evaluation. Furthermore, surface (T_{sur}) and aisle (T_{aisle}) temperatures were included in the assessment. The flow velocities (U) in the occupied passenger zone are an important criterion to evaluate passenger thermal comfort.

In accordance with the thresholds defined in [17], we highlighted temperature deviations smaller than 3.5 K in green, larger than 4.5 K in orange and intermediate values in yellow. Similarly, we used the thresholds indicated in [19] for the evaluation of the local velocities: maximum mean velocities smaller than 1.6 m/s are green, values larger than 3.1 m/s are red and intermediate values are yellow.

Using the comfort sense system, we measured and calculated the predicted mean vote (PMV) and the predicted percentage of dissatisfied (PPD). The PPD is calculated based on the PMV value [17]. The latter itself is an integral

Table 2 Evaluation parameters with measuring explanation

Abbreviation	Explanation
T_{in}	Supply air temperature-averaged value of 72 RTDs in supply ducts
T_{out}	Exhaust temperature-averaged value of 16 RTDs in exhaust pipes
T_{cab}	Mean cabin temperature-averaged value measured by 40 RTDs in row 4 at ankle, knee, chest and head level
T_{amb}	Ambient temperature-temperature in the gap behind the inner surfaces, i.e., temperature of the aluminum sheets of the capillary tubes
T_{chest} (ΔT_{chest})	Temperature at chest level for 60 RTDs—one for each TM in rows 3–8 Temperature difference between maximum and minimum value at chest level
T_{aisle}	Temperatures measured by sensor rack (SR3) in aisle section at 12 height levels
$\Delta T_{h\text{-}a}{}^{seat}$	Maximum temperature gradient on a seat between head and ankle in row 4 and 6
ΔT^{max}	Temperature variation in the occupied zone: difference between the maximum and the minimum temperature of all sensors in row 3–8
T_{sur}	Surface temperatures measured with infrared thermography
U	Velocity measured in row 6 for ten seats at aisle, knee, chest and head level
HRE	Heat removal efficiency calculated using T_{in}, T_{out}, T_{cab}
AoA	Age of air
PMV	Predicted mean vote
PPD	Predicted percentage of dissatisfied

thermal comfort quantity and comprises air temperature, radiation temperature, air velocity and humidity. For the PPD index, all values PPD < 15% are marked in green, 15% < PPD < 30% in yellow, 30% < PPD < 50% in orange and PPD values exceeding 50% are marked in red. For PMV representing the temperature evaluation on a scale from − 3 (too cold) via 0 (neutral) to + 3 (hot), this corresponds to green values for |PMV| < 0.8, yellow values for 0.8 < |PMV| < 1.0 and the extreme conditions in orange and red in accordance with the thresholds stipulated in [18].

Finally, we calculated the heat removal efficiency (HRE $= 0.5 \cdot \left(T_{\text{out}} - T_{\text{in}}\right) \cdot \left(T_{\text{cab}} - T_{\text{in}}\right)^{-1}$), which is a measure for the efficiency of the ventilation system. A perfect mixing in the cabin, i.e., $T_{\text{cab}} = T_{\text{out}}$, results in an HRE of 0.5. In this case green ($0.5 \leq$ HRE) corresponds to a good rating with T_{out} being at least equal or higher compared to T_{cab}. Yellow ($0.3 \leq$ HRE < 0.5) represents an acceptable value, while red (HRE < 0.3) indicates a non-efficient ventilation system in terms of heat removal capability. State-of-the-art MV concepts reach HRE values of about 0.4, see [15]. A higher HRE value of a ventilation system represents a more efficient removal of the heat from the cabin by the airflow. In single-aisle aircraft, novel ventilations concepts, such as cabin displacement ventilation or a hybrid ventilation concept, revealed much higher HRE values compared to state-of-the-art MV [15]. Finally, we evaluated the temperature difference between $T_{\text{cab}} - T_{\text{in}}$, which is another possible evaluation criterion for the efficiency of the ventilation system as it is a measure for the required supply air temperature conditions of the HVAC system. For a stationary and comfortable value of $T_{\text{cab}} = 23$ °C and a constant volume flow rate, higher supply air temperatures result in a lower cooling demand for the HVAC system.

4 Experimental results

In this chapter the investigated ventilation concepts will be compared under "norm flow" conditions. In the present paper we focus on the cases with a 50–50% volume flow rate split between the slanted and the straight ceiling outlets for LMCV and MJV as well as a 50–50% split between the lateral and the ceiling supply at MV. Selected results for other volume flow split rates can be found in [19]. Section 4.1 presents the results under normal flight conditions

("Cruise"), while in Sec. 4.2 the scenarios under "HDoG" conditions will be discussed.

Before briefly discussing the results regarding the different ventilation concepts, it should be noted that throughout all tests, the mean cabin temperature (T_{cab}) of 23 °C was maintained by adjusting T_{in}. The mean cabin temperature was calculated using 40 temperature probes positioned on all ten seats in row 4 at four different height levels. This definition ensures comparability.

4.1 Cruise

Table 3 summarizes the averaged values for the supply air (T_{in}), the exhaust air (T_{out}), the mean cabin temperature (T_{cab}) and the ambient temperature (T_{amb}). As previously outlined, T_{in} was regulated to maintain a mean cabin air temperature of $T_{\text{cab}} = 23$ °C in row 4 with deviations as small as 0.1 K. Minor differences of ± 0.8 K were observed for T_{amb}. Another possible evaluation criterion for the efficiency of the ventilation system is the temperature difference between T_{cab} and T_{in}, which is a measure for the requested supply air conditions of the HVAC system. For a stationary and comfortable value of $T_{\text{cab}} = 23$ °C, higher supply air temperatures imply a lower cooling demand for the HVAC system. No major differences were found between the variants.

4.1.1 Air and surface temperatures in the cabin

In this chapter the temperatures for all investigated flow distributions under "Cruise" conditions will be discussed. Figure 5 shows the temperatures in the vicinity of the TMs at four height levels (ankle, knee, chest, head) as boxplots. The temperatures at the ankle show no major differences depending on the ventilation system. Mean values between 21.4 and 21.8 °C were found for the different configuration. MJV show the smallest temperature variations (21.3–22.3 °C), LMCV, in contrast, revealed an increased range between 20.6 and 22.3 °C.

At knee height, the results show similar mean values and very little spreading of the data points for all ventilation systems.

However, single outliers, i.e., measured data from single seats outside the 1.5 inter quartile range, were found for all cases. It has to be noted that these outliers show a maximum temperature difference of 0.4 K compared to the

Table 3 Test cases for the investigated ventilation systems under "Cruise" conditions with a volume flow of 1000 l/s

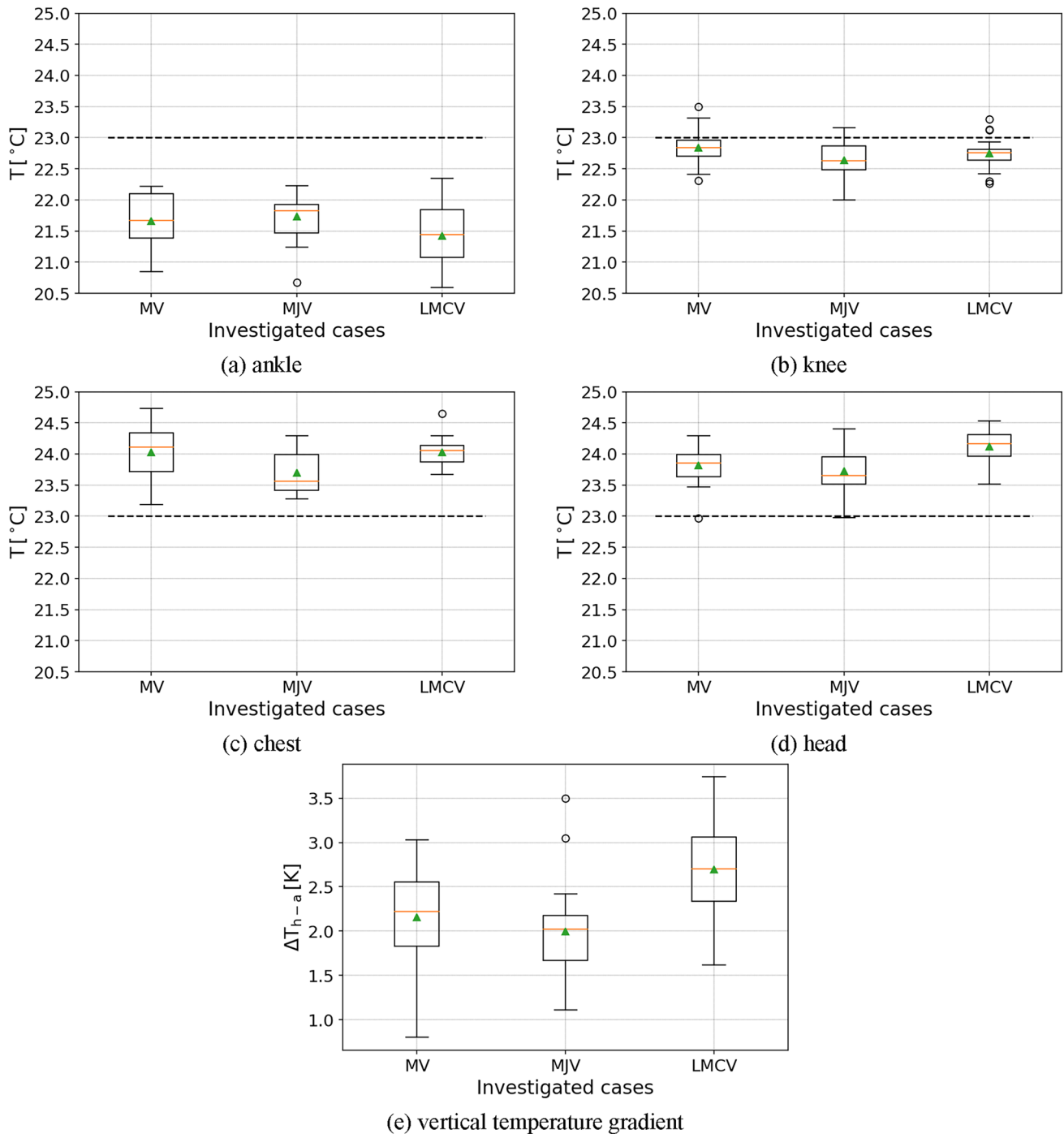| Case	Exhaust	Q_{V}^{1} [l/s]	Q_{V}^{2} [l/s]	T_{cab} [°C]	T_{amb} [°C]	T_{in} [°C]	T_{out} [°C]	$T_{\text{cab}} - T_{\text{in}}$ [K]
MV	Dado	500 (ceiling)	500 (lateral)	23.1	11.6	18.8	21.2	4.3
MJV		500 (slanted)	500 (straight)	23.1	11.4	18.6	21.3	4.5
LMCV				23.0	10.1	18.4	21.0	4.6

Fig. 5 Boxplots of fluid temperatures in the vicinity of the TMs for the investigated cases at **a** ankle, **b** knee, **c** chest, **d** head level and **e** vertical temperature gradient. Orange line: median, green triangle: mean, box: from lower to upper quartile (=inter quartile range IQR), whiskers: farthest data point lying within $1.5 \times$ IQR. The black line at 23.0 °C in **(a)**–**(d)** reflects the mean cabin air temperature (T_{cab})

mean temperature. They are only marked as outliers due to the very low spreading of the values on the other seats and thus a very small inter quartile range. At chest level, the largest range of data and whiskers for MV was discovered. The differences amount to a maximum of 1.5 K. From MV to LMCV, the range of data and the whiskers decrease

to a minimum temperature difference of 0.6 K. Except for one seat in case of LMCV, no outliers were found. At head level, minor differences were detected between the examined ventilation systems, see Fig. 5d. Apart from one outlier for MV, the largest range of data and whiskers was observed at MJV. MV and LMCV show similar results

shifted by 0.5 K. Small differences between the mean head and ankle temperatures, that is, always less than 3 K, were found in row 4 and 6 for all systems. Finally, Fig. 5e shows a boxplot of the vertical temperature gradient between head and ankle for all measuring positions in row 4 and 6. The mean temperature increases from 2.0 K for MJV via 2.2 K for MV to 2.7 K for LMCV. Except of MJV with lower values, the ranges from lower to upper quartiles as well as the whiskers do not change significantly under MV and LMCV conditions. However, two outliers were found at MJV.

The average temperatures per row (averaged at chest height in the cross section) do not show any major differences in longitudinal direction, see Fig. 6a. In general, it should be noted that spatial temperature differences of 2.5 K or less are all rated as good [16]. The averaged values in longitudinal direction (Fig. 6b) reveal lower temperatures for window (A, K) and aisle (C, H) seats as compared to the middle seats (B, E, F, J) on both sides of the cabin for all systems. Despite a set T_{cab} of 23 °C, Fig. 6b shows temperature differences at chest level of up to 1.0 K. The vertical temperature gradient in the aisle region is depicted in Fig. 6c. A higher temperature stratification caused by MV

was repeatedly observed. The best result with a temperature stratification below 1 K was achieved with MJV and LMCV.

Figure 7 shows the chest temperatures in row 3–8 in the vicinity of the TMs as contour plots from above. The largest temperature difference of up to 2.5 K can be found for MV. All ventilation scenarios show approximately the same temperatures in flight direction right (FDR) compared to flight direction left (FDL). However, the temperature distributions show large differences between MV and the novel ventilation systems. While the warmest places for MV are in the middle of the cabin, MJV and LMCV show a longitudinal temperature increase.

In order to discuss the influence of the flow distribution on the surface temperatures, the differences at the inner surfaces were recorded at the side panels, see Fig. 8. For all concepts we found decreased surface temperatures in the first and the last rows. They result from the front and rear boundary walls in combination with missing heat loads in these areas. Consequently, we excluded the first two and the last two rows from further evaluation in the following chapters of the manuscript. Nevertheless, besides this temperature drop in the front and the rear, a rather homogeneous surface temperature distribution was found for MV, see Fig. 8a,
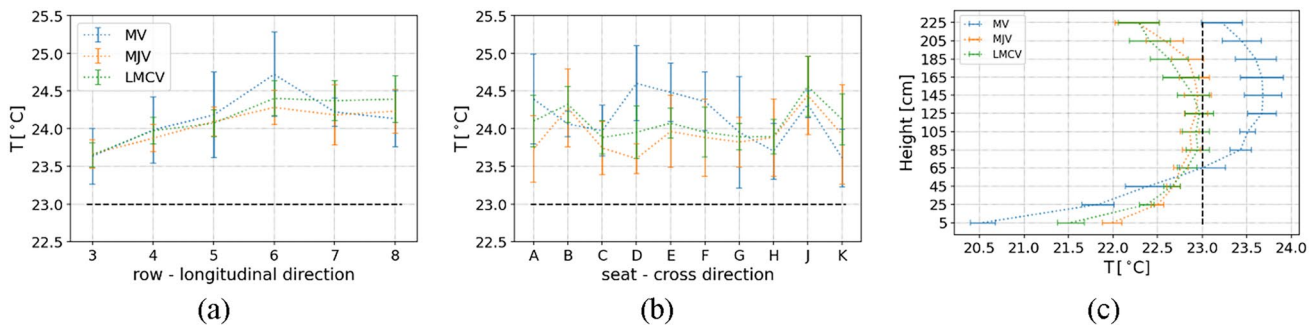

Fig. 6 Fluid temperatures at chest position of the TMs in row 3–8 averaged over **a** seat rows, **b** seat columns as well as **c** for the aisle position for the investigated cases under "Cruise" conditions. The black line at 23.0 °C reflects the mean cabin air temperature (T_{cab})
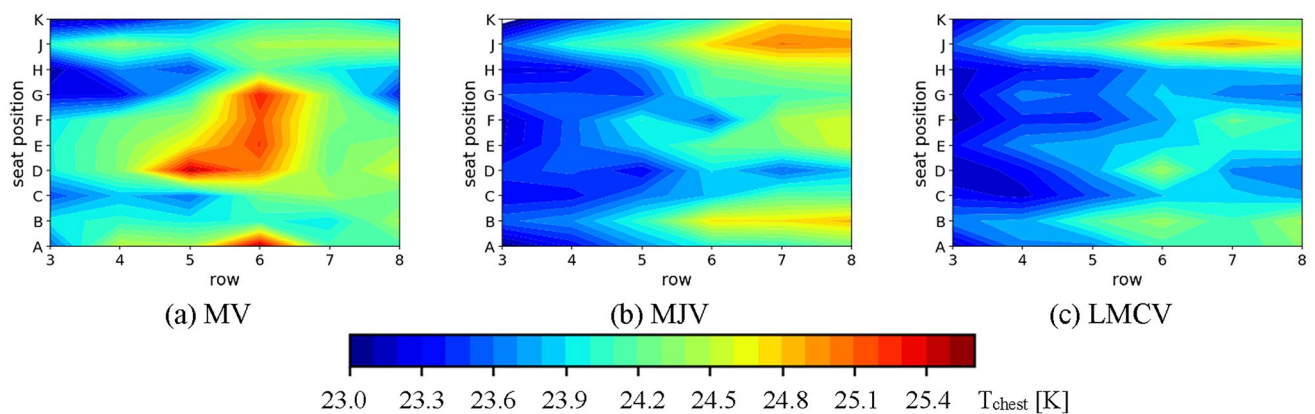

Fig. 7 Contour plot of 60 chest temperatures measured in row 3–8 for **a** MV, **b** MJV and **c** LMCV under "Cruise" conditions
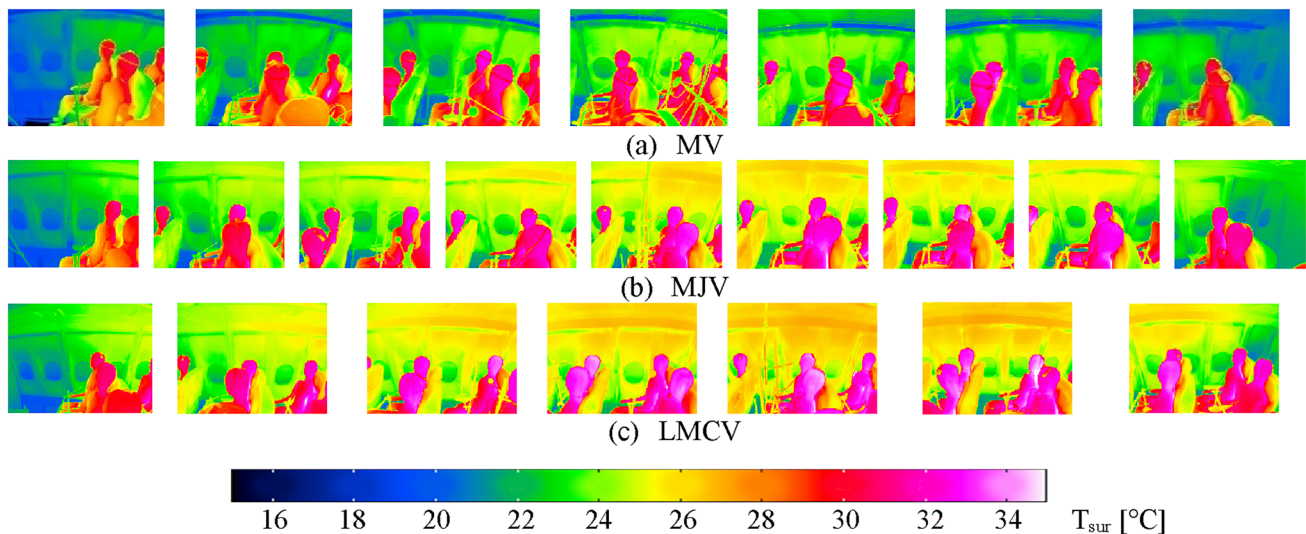
Fig. 8 Surface temperatures of the panels measured (in FDR) with infrared thermography for **a** MV, **b** MJV and **c** LMCV under "Cruise" conditions

revealing temperatures around 2324 °C. In case of MJV (b) and LMCV (c), the temperatures at the sidewalls were higher (up to 27 °C) and show a stronger variation. We attribute this effect to less forced airflow in the sidewall area as the supply air openings for both alternative concepts are in the aisle region only. Consequently, the impact of the thermal stratification induced by the heat release of the thermal passenger manikins is more prevalent and thus results in more inhomogeneous temperature distributions on the sidewalls.

4.1.2 Comfort-relevant local air velocities

Figure 9 depicts the mean fluid velocities in row 6 at ankle, knee, chest and head level at a volume flow rate of $Q_V = 1000$ l/s. The first thing to note is that no high mean velocities averaged over 1800 s greater than 0.31 m/s—outbalancing the maximum velocity as upper comfort threshold defined in [20]—were found for any measurement position or ventilation system. Very low velocities and fluctuations were observed at the ankle for FDL. In FDR, particularly close to the aisle, slightly increased values were found-primarily for MV and LMCV. Slight differences were found on the left and right at knee height with fluctuations reaching up to 0.16 m/s. The highest velocities for MJV and LMCV were measured at the lower part of the body. This changes for the upper body. In front of the chest, the values for MV increase significantly, but are still well below the maximum of 0.31 m/s. Due to the horizontal lateral inflow, the highest velocities were found in the middle segment at head level for MV. Except seat 6G at head level, the fluctuations do not exceed this limit. A homogeneous distribution in the cross section was found for all systems.

Figure 10 shows the boxplots of the velocities at different heights in the vicinity of the TMs. At ankle level, almost no air movements were measured. Slightly higher velocities with a mean value lower than 0.15 m/s were found for LMCV. The same levels could be observed at knee height. MV generates the longest whiskers up to 0.2 m/s. Under LMCV conditions, an outlier was detected at 0.18 m/s. In addition, no values higher than 0.23 m/s were found at chest height (c). MJV and LMCV generate a wide range of data. Finally, Fig. 10d shows the velocities at head height as a boxplot. They do not differ significantly from the chest values. The whiskers also show no values above 0.25 m/s. A comprehensive presentation of all velocities in one boxplot, see Fig. 10e, shows a decrease in median, mean value, lower to upper quartile as well as regarding the whiskers from MV to MJV to LMCV. Based on the upper threshold of 0.31 m/s in accordance with [20], all values were classified as non-critical.

4.1.3 Air quality: CO$_2$ concentration and age-of-air

Figure 11 shows boxplots of the CO$_2$ concentrations above the background concentration, that is, the CO$_2$ concentration in the supply air, (left) as well as the age of air (AoA) (right) under "Cruise" conditions. It should be noted that the cases examined were all operated with fresh air. With a CO$_2$ enrichment of 4% during human respiration and a breathing rate of 6 l/min, an expected average increase of the CO$_2$ concentration of 400 ppm can be calculated. The lower observed values in the cabin are expected to be a result of the measuring positions of the CO$_2$ sensors (Fig. 2 left), i.e., it seems that the exhausted CO$_2$
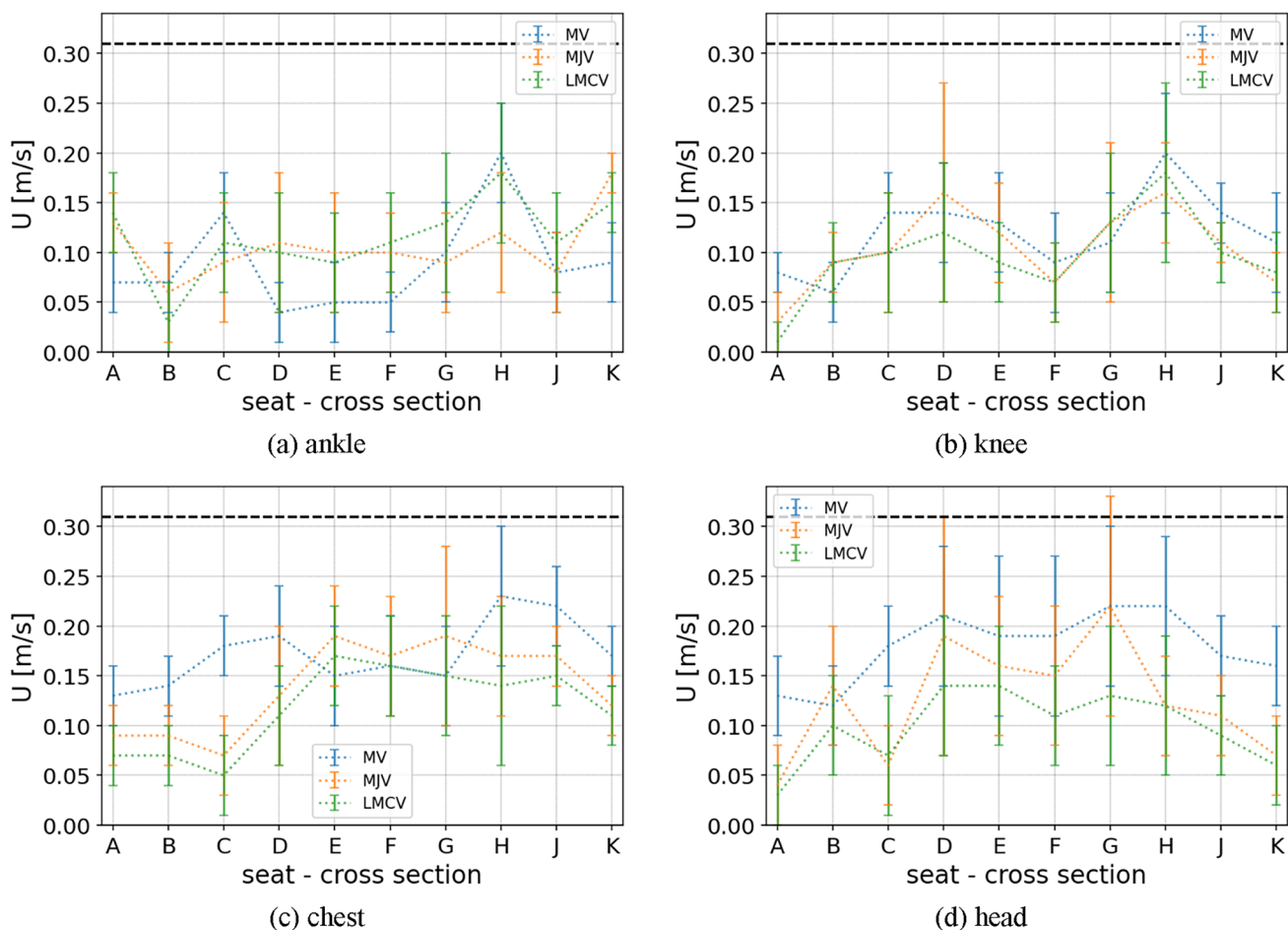
Fig. 9 Comparison of the fluid velocities in the vicinity of the TMs for the investigated cases at **a** ankle, **b** knee, **c** chest and **d** head position. The black line at 0.31 m/s reflects the upper comfort threshold in accordance with [20]

is only reaching the sensor position with low concentrations. In other words, the air in the cabin in not perfectly mixed and the sensors seem to be in areas with rather fresh air. In future measurements, it should be considered to increase the number of sensors and to add CO_2 sensors in the exhaust air. Further, it should be noted that the CO_2 concentrations in a real aircraft in operational mode will be higher compared to our reported values due the recirculation air with amounts typically to about 50% of the total air flow. Nevertheless, for both, the calculation of the ventilation performance in terms of the age of air and the comparison of the recorded absolute values between the different concepts, our approach with 100% fresh air supply is reasonable. It is obvious that all investigated ventilation systems are able to generate only low CO_2 concentrations within the cabin. The parameter AoA reveals mean values as low as 2.8–3.3 min for all sidewall- and ceiling-mounted ventilation systems. Ranking the investigated ventilation system based on the results of the tracergas measurements, the LMCV system performs well and

is absolutely comparable to the MV system. However, the best results could be observed with the MJV system.

4.2 Hot day on ground

Table 4 contains the averaged values for the supply air (T_{in}), the exhaust air (T_{out}), the mean cabin (T_{cab}) as well as for the ambient temperature (T_{amb}) under "HDoG" conditions. In addition, the difference between T_{cab} and T_{in} was calculated in order to assess the system. Slight differences of 1.9 K, which are not decisive, were observed for T_{amb}. Based on the temperature difference between $T_{cab}-T_{in}$, the best results were found for MJV.

4.2.1 Air and surface temperatures in the Cabin

Figure 12 shows boxplots of the temperatures in the vicinity of the TMs at four height levels (ankle, knee, chest, head). First of all, it should be noted that no significant deviations from the standard were found.
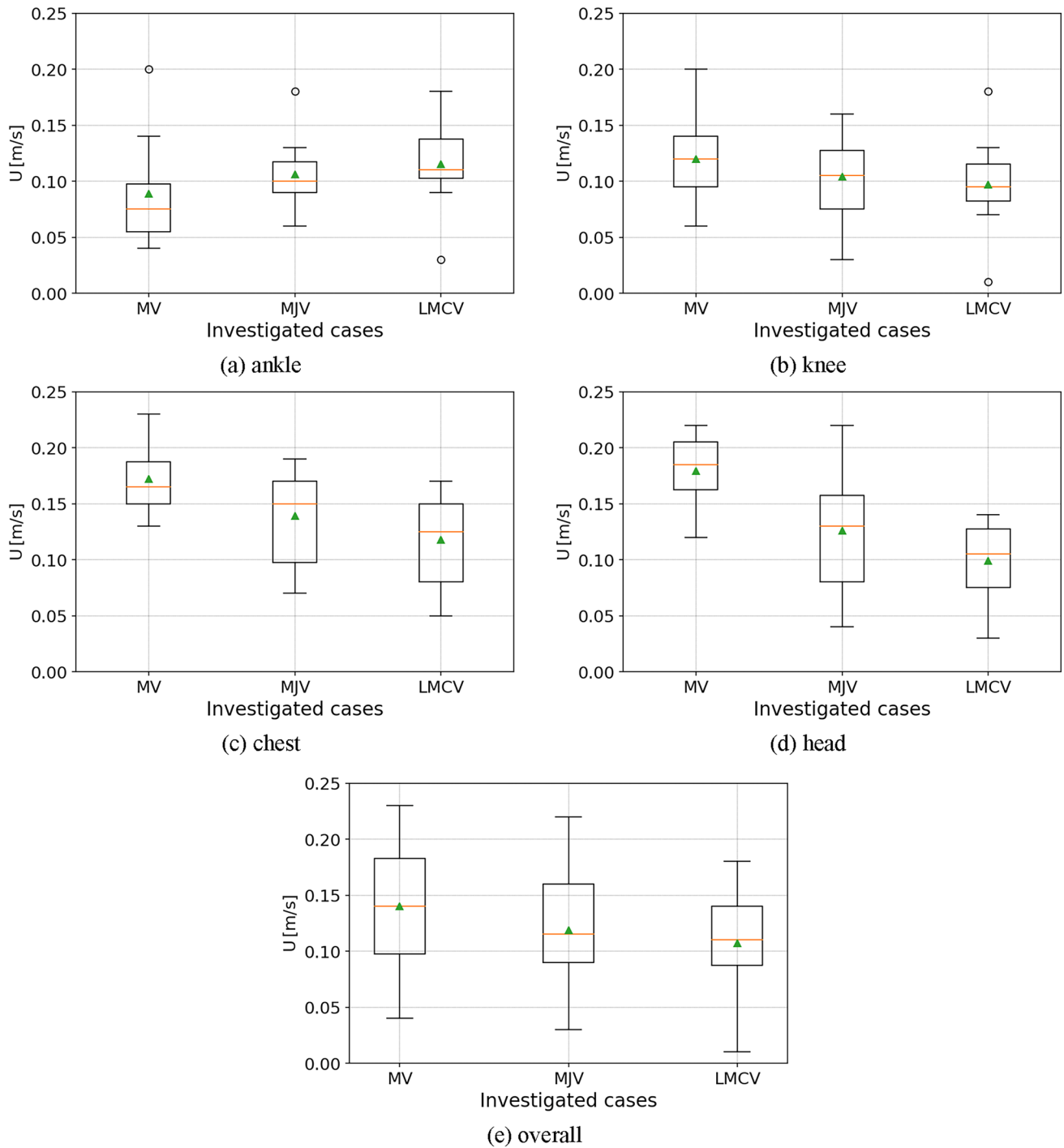
Fig. 10 Boxplots of the fluid velocities in the vicinity of the TMs for the investigated cases at **a** ankle, **b** knee, **c** chest, **d** head level and **e** for all body positions. Orange line: median, green triangle: mean, box: from lower to upper quartile (=inter quartile range IQR), whiskers: farthest data point lying within $1.5 \times$ IQR

For MV, temperatures close to the mean cabin temperature ($T_{cab} = 23.0$ °C) were observed at all height levels. For MJV and LMCV, a temperature increase with measurement altitude was found. At ankle height, the largest range of data was found for MV as compared to the alternative ventilation systems (MJV and LMCV), which show similar results. However, shorter whiskers, i.e., less distributed values, were observed from MV to MJV to LMCV. No outliers were detected for all ventilation variants at ankle height. At knee level, the largest temperature differences
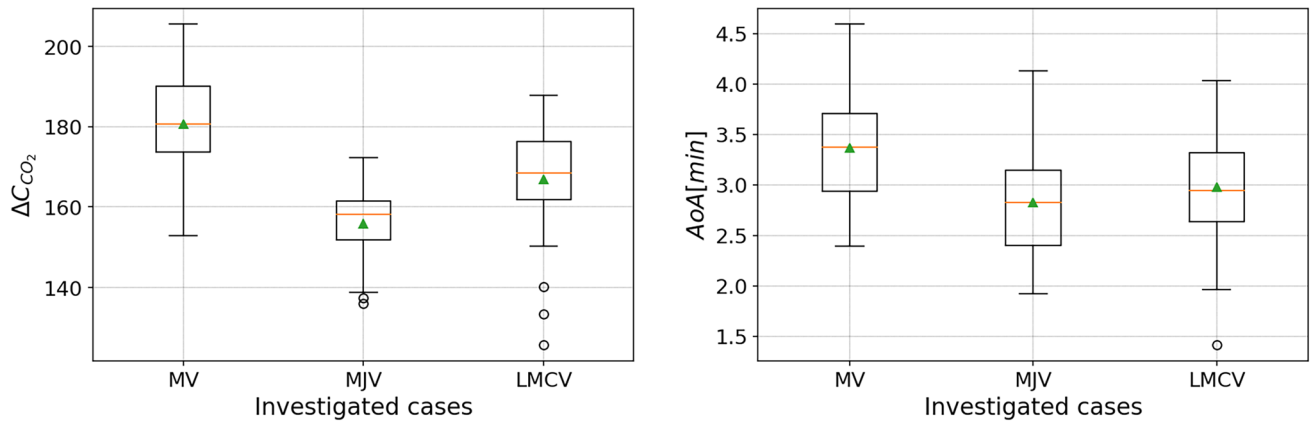
Fig. 11 Boxplot of the CO2 concentrations minus the basis concentration (left) as well as AoA (right) under "Cruise" conditions. Orange line: median, green triangle: mean, box: from lower to upper quartile (= inter quartile range IQR), whiskers: farthest data point lying within 1.5×IQR

Table 4 Investigated test cases for the ventilation systems under "HDoG" conditions

Case	Exhaust	$Q_V{}^1$ [l/s]	$Q_V{}^2$ [l/s]	T_{cab} [°C]	T_{amb} [°C]	T_{in} [°C]	T_{out} [°C]	$T_{cab}—T_{in}$ [K]
MV	Dado	500 (ceiling)	500 (lateral)	22.9	33.1	13.1	23.0	9.8
MJV		500 (slanted)	500 (straight)	23.1	35.0	16.3	22.5	6.8
LMCV				23.1	35.0	14.2	22.7	8.9

of 1.8 K were observed for MV. All systems show a range of data of less than 1.0 K. The best homogeneity with the lowest temperature range could be achieved by MJV and LMCV. At chest level, MV shows the largest range of temperatures amounting to 2.2 K. At this measurement height, lower values were found at LMCV and lowest at MJV. However, the temperatures increase from MV to MJV to LMCV. Similar results were found for the head temperatures with maximum temperature differences of 2.7 K at 20 seats in cross section caused by a maximum and minimum outlier under MJV conditions.

Only a few outliers were recorded for all cases and heights. Unlike the "Cruise" case, the boxplot of the vertical temperature gradient between head and ankle shows the maximum values for LMCV followed by MJV and the lowest values for MV. However, for the temperatures from lower to upper quartiles, the smallest differences occurred for MJV and LMCV, while MV shows a temperature range of 1.2 K. Maximum temperature differences of 2.9 K for MV also show the good rating of all systems.

The values averaged over the cross section and plotted in longitudinal direction in Fig. 13a show the temperature increase from row 3 to row 8 for all systems. All systems are very similar up to row 4. However, towards the rear, temperature differences of upto 1.5 K occurred. The standard deviations show no significant differences. MV exhibits the most homogeneous distribution with differences

smaller than 1.4 K. The largest horizontal temperature difference of 2.4 K is found for LMCV.

The mean temperature values in longitudinal direction relative to T_{cab} are shown in Fig. 13b for the cross section. MJV and LMCV show a similar temperature curve with generally higher values on the middle seats (B, E, F, J). For MV, temperature differences were found from FDR to FDL with chest temperatures below T_{cab} in FDR. As in a), Fig. 13c shows similar temperature profiles in the passage area for all systems. Following the increase in temperature with decreasing height in the ceiling area (above 185 cm), constant values were recorded between 185 and 65 cm. Below this height, the values also increase slightly. However, none of the temperature stratifications are to be regarded as critical either.

Figure 14 shows the chest temperature in the vicinity of the TMs as a contour plot from above. First of all, it should be noted that none of the systems can achieve a homogeneous temperature distribution in the entire cabin. As already indicated in Fig. 13a, all cases show lower temperatures on all seats in the front rows. In contrast to the temperature layers (head-ankle), higher but acceptable values could be found at chest level, see Table 6. Based on the FDL-FDR homogeneity, LMCV shows the best values. MJV results in the lowest maximum differences, see Table 6.

In order to discuss the influence of the flow distribution on the surface temperatures, infrared views of FDR are
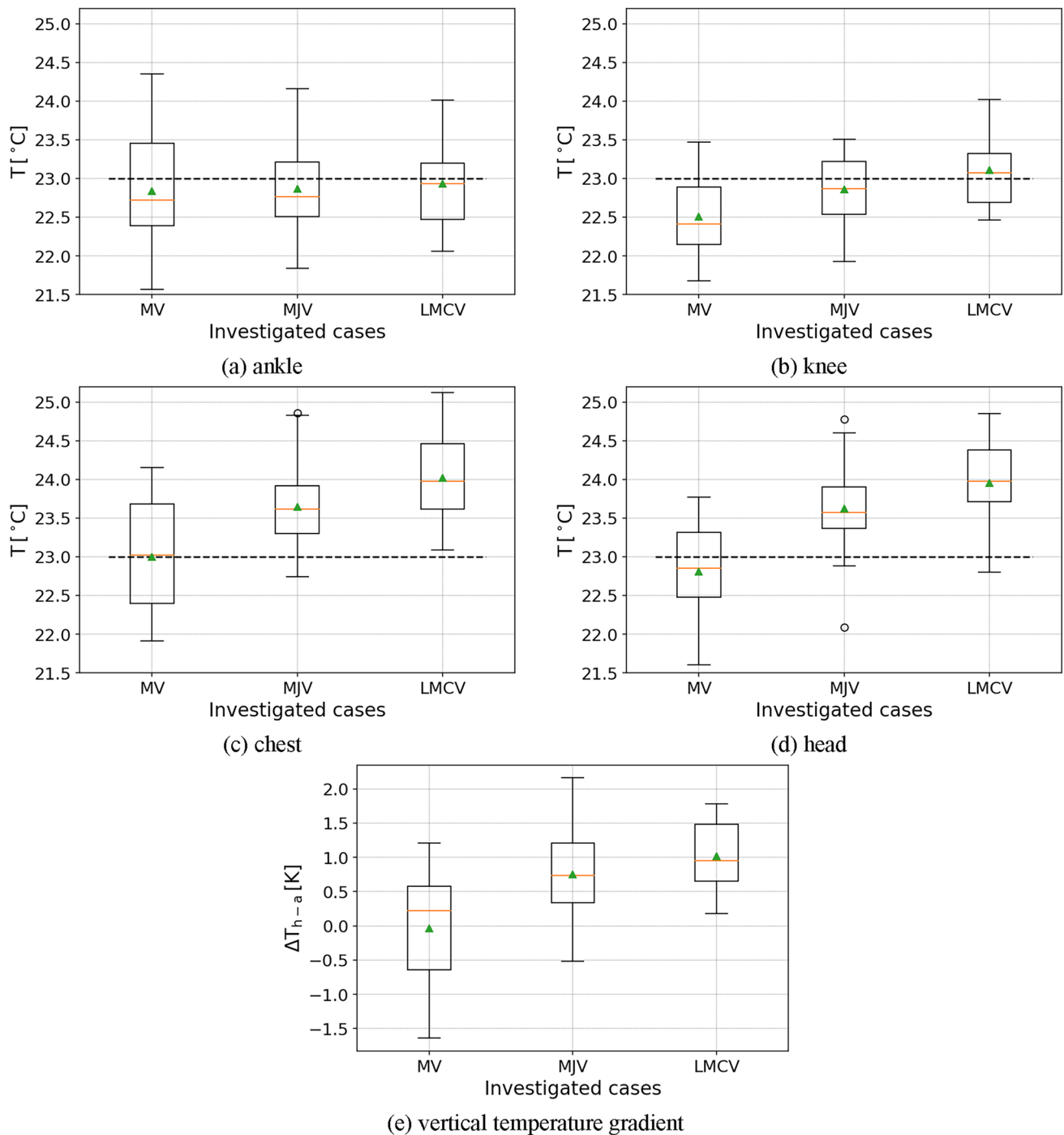
Fig. 12 Fluid temperatures in the vicinity of the TMs for "HDoG" conditions at **a** ankle, **b** knee, **c** chest, **d** head level and **e** the vertical temperature gradient. Orange line: median, green triangle: mean, box: from lower to upper quartile (=inter quartile range IQR), whiskers: farthest data point lying within 1.5×IQR. The black line at 23.0 °C in (**a**)–(**d**) reflects the mean cabin air temperature (T_{cab})

presented in Fig. 15 corresponding to the cruise images presented in Fig. 8. For MV, see Fig. 15a, we again see rather homogeneous surfaces temperatures except for the areas in the front and the rear of the cabin. Additionally, the lateral supply air openings below the luggage compartments are shown as dark blue areas at the upper end of the infrared views. For MJV, see (b), a similar surface temperature distribution is found compared to MV, however, without the cold regions of the MV supply air openings. In contrast, LMCV, see (c), reflects much higher surface temperatures compared to the other two concepts, especially in the rear rows, i.e., images 5–8. Since the gap
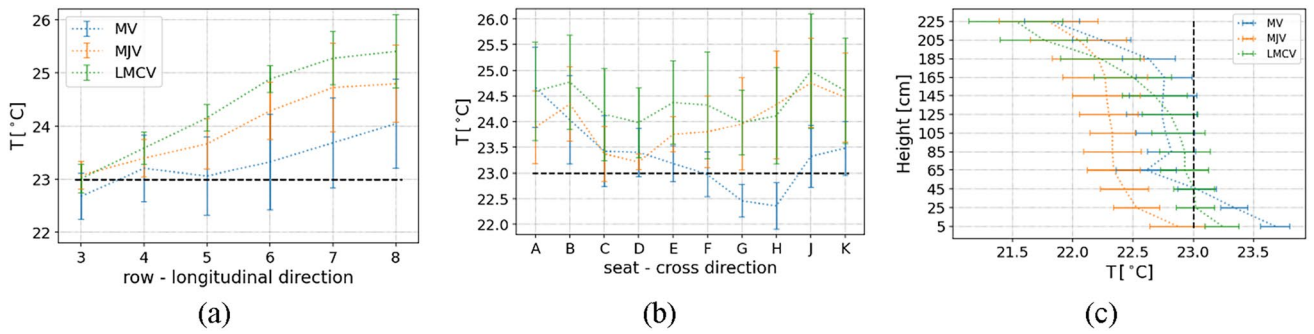
Fig. 13 Fluid temperatures at chest position of the TMs in row 3–8 averaged over **a** seat rows and **b** seat columns as well as **c** for the aisle position under "HDoG" conditions. The black line at 23.0 °C reflects the mean cabin air temperature (T_{cab})
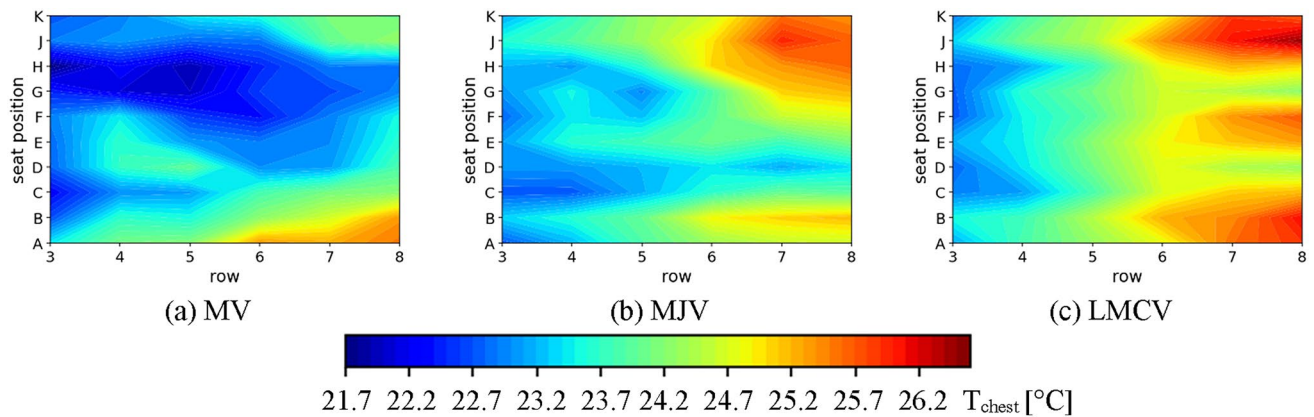

Fig. 14 Contour plot of 80 chest temperatures in row 3–8 for **a** MV, **b** MJV and **c** LMCV under "HDoG" conditions
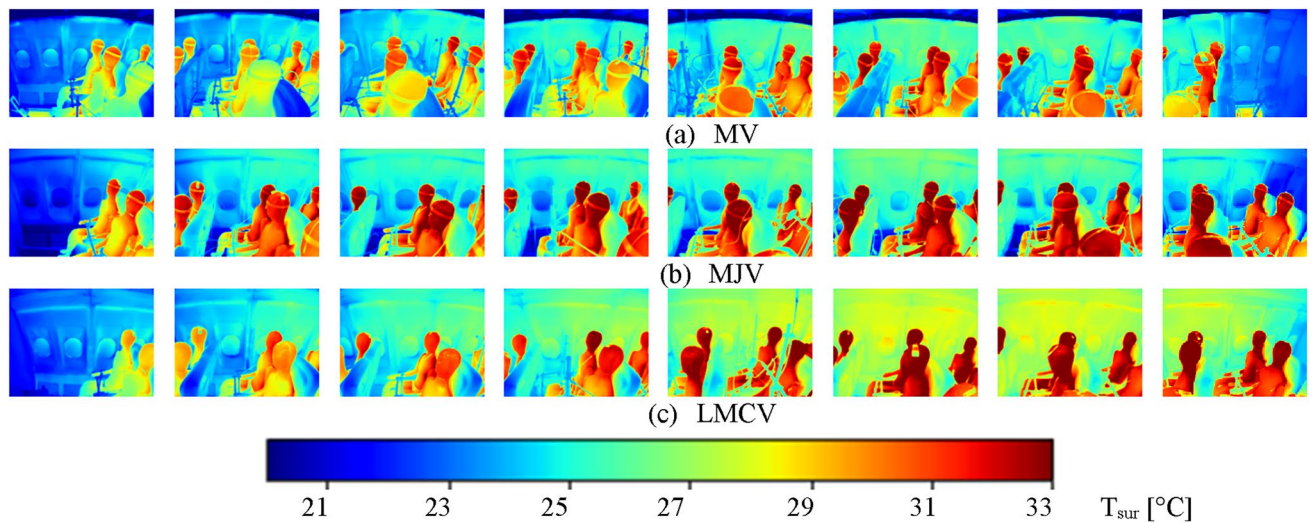

Fig. 15 Surface temperatures of the panels in FDR measured with infrared thermography for **a** MV, **b** MJV und **c** LMCV under "HDoG" conditions

temperatures are maintained at the same level for all concepts, the higher temperatures of the inner surfaces must be a result of different airflow patterns in the cabin. Apparently, in case of LMCV less cold air reaches the lateral

sidewalls and thus higher temperatures are recorded. They might have an effect on the thermal comfort of the adjacent seats, i.e., mainly the window seats, and furthermore, the amount of heat transported through the sidewalls might change.
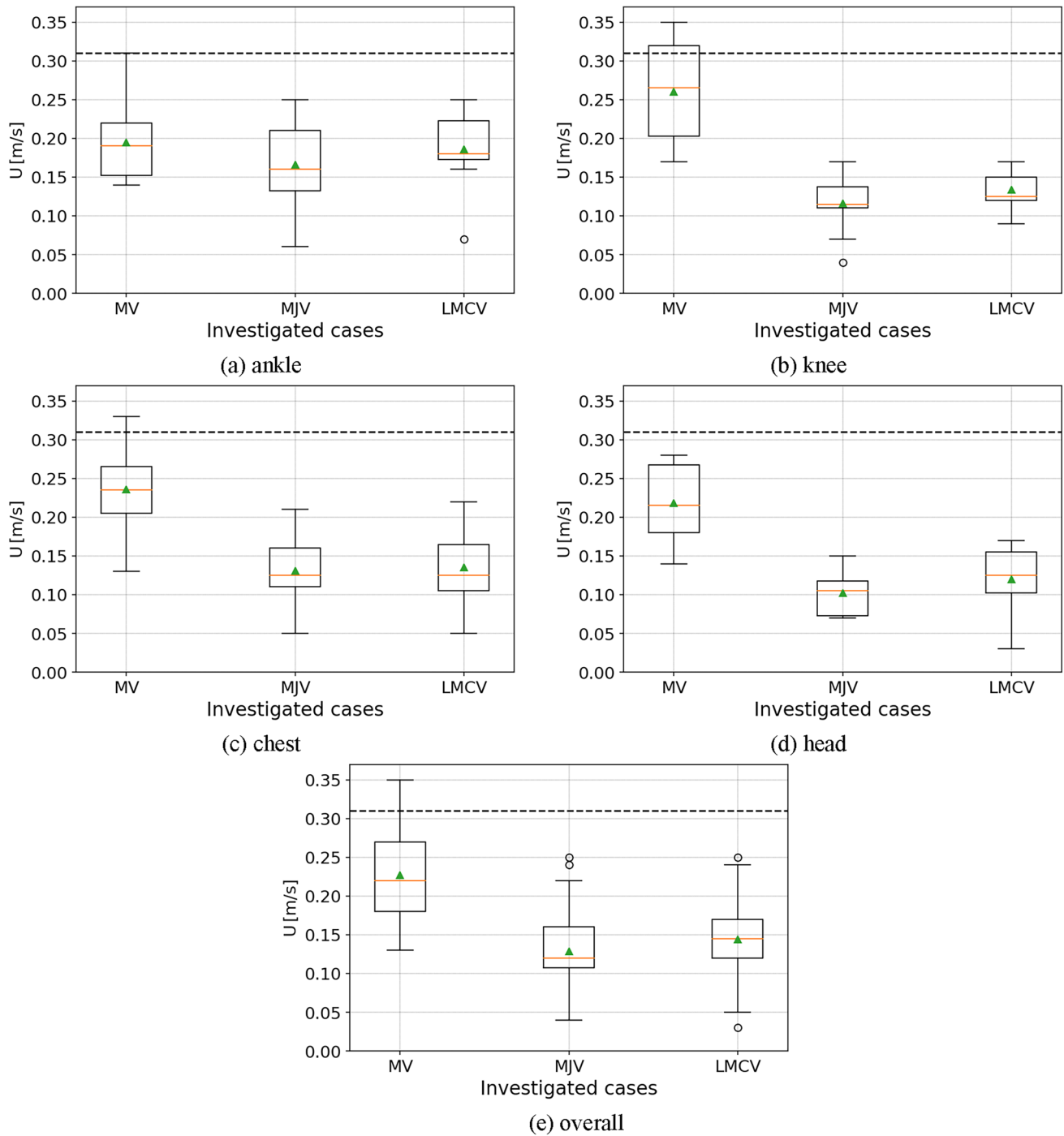

Fig. 16 Comparison of fluid velocities in the vicinity of the TMs for the investigated cases at **a** ankle, **b** knee, **c** chest, **d** head level and **e** for all body positions. The black line at 0.31 m/s reflects the upper comfort threshold in accordance with [20]. Orange line: median, green triangle: mean, box: from lower to upper quartile (= inter quartile range IQR), whiskers: farthest data point lying within 1.5×IQR

4.2.2 Comfort-relevant local air velocities

Figure 16 depicts the mean fluid velocities in row 6 at ankle, knee, chest and head level at a volume flow rate of $Q_V = 1000$ l/s as boxplots. The first thing to note is that for none of these height levels, high mean velocities exceeding 0.31 m/s, were found. This value is defined as upper comfort threshold in [20]. Except for slightly increased whiskers, no major differences between the ventilation systems could be determined at ankle height. For all other heights, the highest velocities were found under MV conditions. The velocities at knee and chest height show similar results for MJV and LMCV with values fluctuating around 0.15 m/s. In case of MV, the data ranges from 0.20 m/s to 0.32 m/s with whiskers up to 0.35 m/s. At head level, which might be the most important position for the evaluation of potentially draft-causing airflows, all values were below the threshold of 0.31 m/s. The distribution between the three concepts was similar regarding ankle and chest height: MV reveals the highest values, whereas the values for MJV and LMCV were on a much lower level. Mean values of 0.21 m/s were found for MV and values of approx. 0.1 m/s were found for MJV and LMCV. With regard to the fluctuations, no clear trend could be identified: LMCV results in the least fluctuations at ankle and knee level, while MJV has a more uniform distribution at head level. In summary, the most important finding of the air velocity analysis is that the alternative ventilation concepts show significantly lower flow velocities compared to MV at all height levels, expect for the ankle position. The averaged velocities across all cases in Fig. 16e show very similar values with 2 outliers for MJV and for LMCV. Slightly increased values were found for MV, with the median and mean being well below the limit of 0.31 m/s specified in [20].

4.2.3 Air quality: CO_2 concentrations and age-of-air

Figure 17 shows the CO_2 concentrations and the age-of-air values of the three different ventilation concepts under hot-day-on-ground conditions as boxplot representations. The first fact to be noted is that the differences between the concepts are rather small for both CO_2 concentration and AoA. In detail, we found slightly higher CO_2 values for MV compared to the other two concepts. Here the average CO_2 concentration minus the basic concentration was around 20 ppm or around 10%. Higher values were found for MV compared to MJV and LMCV. The mean AoA values did not change significantly for the different concepts. However, we observed that the distribution of the local AoA values becomes wider from MV to MJV to LMCV. The comparison of the CO_2 concentrations and the AoA values between the "Hot-day-on-ground" and "the Cruise" scenario reveals a more homogeneous distribution for hot-day-on-ground, while the trends between the different concepts are maintained.

5 Discussion and conclusion

Micro-jet ventilation (MJV), low-momentum ceiling ventilation (LMCV) and a generic state-of-the-art mixing ventilation (MV) concept were analyzed experimentally in a long-range cabin mock-up under cruise and hot-day-on-ground temperature boundary conditions. The concepts were evaluated in terms of thermal comfort, heat removal efficiency and air quality. In order to evaluate the new ventilation systems, the MV reference case was examined first. Very small temperature gradients between head and ankle below 3.7 K were observed under "Cruise" conditions. Slightly increased velocities were observed near the thermal manikins. However, no high mean velocities greater than 0.31 m/s were
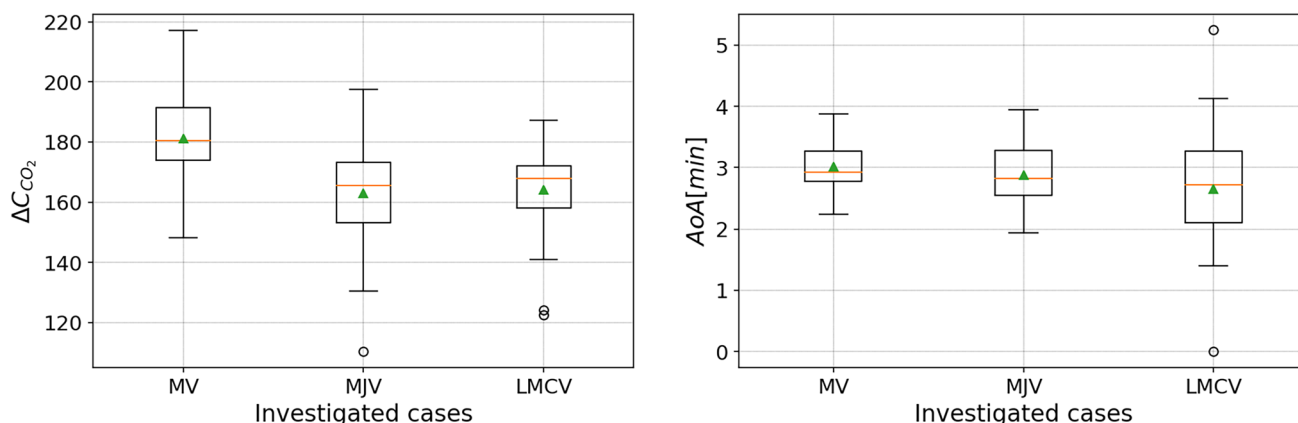

Fig. 17 Boxplot of the CO_2 concentrations minus the basis concentration (left) and AoA (right) under "HDoG" conditions. Orange line: median, green triangle: mean, box: from lower to upper quartile (=inter quartile range IQR), whiskers: farthest data point lying within 1.5×IQR

found. Under "HDoG" conditions increased lateral temperature distributions occurred. Hence, minimizing the velocities close to the seated passengers remains a major challenge. In case of MJV, the complete supply air system can be installed in the ceiling area. In addition to a good fresh air supply for the aisle area, very small temperature gradients were measured both in horizontal and vertical direction. The second novel ventilation system studied in this project was LMCV, where a very similar behavior compared to MJV was found. With the same arrangement of the air outlets and changing the inflow conditions by a low-momentum air supply through planar and large-surface inlets, no major improvements could be achieved.

In the following two tables the main evaluation quantities are summarized for the different concepts under "Cruise" and "HDoG" conditions. The color coding reflects the evaluation as "good" (green), "acceptable" (yellow) and "needs improvement" (orange). The first two columns represent the vertical temperature stratification with the maximum ($\Delta T_{\text{h-a}}^{\text{seat}}$) and mean ($\Delta T_{\text{h-a}}^{\text{mean}}$) difference indicated for 10 seats in row 4 and 6. The difference between the maximum and minimum temperature in the vicinity of the TMs at chest level from row 3 to 8 as well as at 4 height levels (ankle, knee, chest, head) in row 4 and 6 is given as ΔT^{max}. The fourth column reflects the horizontal temperature homogeneity at chest level with maximum and minimum values determined between row 3 and 8. The local velocities in the vicinity of the passengers are depicted in the fifth column. Columns eight represents the heat removal efficiency (HRE). The last two columns summarize the air-quality assessment in terms of the mean local CO_2 concentration with regard to the supply air concentration and the age of air (AoA).

Table 5 shows the main results for the investigated ventilation systems under "Cruise" conditions. No major differences were found between the variants. All temperature gradients between head and ankle (column 1 and 2) as well as the chest temperatures are rated as acceptable in accordance with the requirements defined in the standard [18]. However, looking at the temperature variation in the passenger zone

reveals that the temperature variation increases to 4.4 K for MJV and LMCV and to an exceeding value of 4.7 K for MV. With the aim to achieve perfect mixing of fresh and cabin air caused by the fast inflow velocities from both sides of the cabin, low velocities could be generated by evenly distributing the volume flow (50–50) for all systems. Based on [20] acceptable values could even be measured for MV. No differences were found in relation to the heat removal efficiency (HRE). Perfect mixing in the cabin, i.e., $T_{\text{cab}} = T_{\text{out}}$, would result in an HRE of 0.5. All ventilation systems show very promising tracer gas results.

Further, the results under "HDoG" conditions are shown in Table 6. For the vertical temperature gradient between head and ankle, almost no stratification was found and all systems were rated as good, see columns 1 and 2. All temperature gradients meet the requirements defined in the standards [16, 20]. However, ΔT_{chest} shows slightly increased horizontal temperature variations for all ventilation concepts with a minimum of 3.3 K for MJV up to 3.8 K for LMCV and MV. Considering all sensors in the vicinity of the TMs, the temperature variation increases from MV (4.0 K) via MJV (4.1 K) to a maximum of 4.4 K at LMCV. As shown under "Cruise" conditions, low and acceptable velocities were found for all systems by evenly distributing the volume flow in accordance with [20]. As expected and already observed in the "Cruise" cases, the systems do not generate a large ΔT between T_{out} and T_{in}, which is reflected in a low HRE. However, MV with floor-based air exhaust results in a large temperature difference and, thus, a good HRE. The overview of the investigated CO_2 measurements shows that all systems deliver very promising results.

Additionally, the thermal comfort on seat 6 J was evaluated using the PMV and PPD index, see Table 7. It summarizes the mean, maximum and minimum PMV values as well as the mean and worst PPD evaluations. Please note that these values were only directly measured on seat 6 J, as shown in Fig. 2 (left). For the evaluation of the mean values in the cabin, we assumed a constant radiant temperature—as determined on seat 6 J—and used the local values of the air

Table 5 Temperature evaluation parameters for the investigated cases under "Cruise" conditions

Case	$\Delta T_{\text{h-a}}^{\text{seat}}$ [K]	$\Delta T_{\text{h-a}}^{\text{mean}}$ [K]	ΔT^{max} [K]	ΔT_{chest} [K]	$\langle U \rangle_{\text{max}}$ [m/s]	HRE [-]	Δc_{CO_2} [ppm]	AoA [min]
MV	3.0	2.2	4.7	2.5	0.23	0.28	180.6	3.37
MJV	3.5	2.8	4.4	2.2	0.22	0.30	155.8	2.82
LMCV	3.7	3.0	4.4	1.6	0.18	0.28	166.5	2.97

Table 6 Temperature evaluation parameters for the investigated cases under "HDoG" conditions

Case	$\Delta T_{\text{h-a}}^{\text{seat}}$ [K]	$\Delta T_{\text{h-a}}^{\text{mean}}$ [K]	ΔT^{max} [K]	ΔT_{chest} [K]	$\langle U \rangle_{\text{max}}$ [m/s]	HRE [-]	Δc_{CO_2} [ppm]	AoA [min]
MV	1.2	0.3	4.0	3.8	0.35	0.51	182.3	3.02
MJV	1.9	1.2	4.1	3.3	0.28	0.46	163.0	2.88
LMCV	1.8	1.0	4.4	3.8	0.25	0.48	164.8	2.64

Table 7 PMV and PPD comfort evaluation on seat 6 J and extrapolated to the other seats using a constant T_{rad}

Case	Scenario	Seat 6J					All (extrapolated)				
		PMV [−]			PPD [%]		PMV [−]			PPD [%]	
		mean	*max*	*min*	*mean*	*worst*	*mean*	*max*	*min*	*mean*	*worst*
MV	cruise	-0.46	-0.39	-0.58	9.3	11.9	-0.42	-0.24	-0.62	8.6	13.1
	HDoG	-0.65	-0.60	-0.76	13.8	17.3	-0.68	-0.49	-0.86	14.8	20.5
MJV	cruise	-0.06	-0.01	-0.12	5.1	5.3	-0.15	0.05	-0.47	5.5	9.6
	HDoG	0.16	0.24	0.07	5.5	6.2	0.01	0.28	-0.51	5.0	10.4
LMCV	cruise	-0.08	-0.01	-0.14	5.1	5.4	-0.12	0.01	-0.32	5.3	7.1
	HDoG	0.17	0.24	0.10	5.6	6.2	0.06	0.31	-0.25	5.1	7.0

temperature and air velocity for the calculation of the PMV and PPD values for all other seats in row 6. We assumed a clothing value of clo = 0.85, corresponding to a seated person wearing long trousers and a long-sleeve shirt in accordance with ISO7730 [18].

All investigated cases except MV under HDoG conditions provide good values of PPD < 15% and |PMV| ≤ 0.7 according to [18]. However, most of the values are slightly below zero, indicating that $T_{cab} = 23$ °C in combination with the radiant temperatures of the surrounding walls and the local air velocities are rated as slightly cool (but comfortable). The only values below the lower threshold for good conditions are found in case of MV under HDoG conditions. For seat 6 J, they result from increased local velocities at chest position 6 J (0.27 m/s) at rather low air temperatures of 22.6 °C, while the worst overall evaluation was determined at the knee position of seat 6D, where an air velocity of 0.35 m/s at a temperature of 22.2 °C was measured.

Despite these slightly critical local values, the overall thermal comfort as determined by PMV and PPD was evaluated as good for all concepts and conditions. Under cruise conditions, the alternative ventilation concepts MJV and LMCV revealed minor advantages with mean PPD values ranging from 5.1 to 5.5 compared to MV, where mean PPD values of up to 9.3 were found. The worst PPD evaluations for these alternative concepts ($PPD_{worst} \leq 9.6$) were about 25% better compared to MV ($PPD_{worst} \leq 13.1$). For the HDoG conditions again, much better PPD values were found for LMCV and MJV compared to MV. However, a closer look at the PMV values—especially at HDoG conditions—reveals that MV was evaluated slightly too cool for all values, whereas LMCV and MJV showed both positive and negative PMV values. As a consequence, an increased mean temperature in the cabin could enhance the evaluation of MV, while LMCV and MJV already seem to be well-balanced around the optimal mean cabin temperature. In addition mixed ventilation is providing higher velocities due to its higher momentum forces. Furthermore, we found a slightly larger variation of the PMV values for the alternative concepts ($\Delta PMV \leq 0.79$) compared to MV ($\Delta PMV \leq 0.38$).

It can be concluded that a simple "one-optimizing-all-challenges" ventilation concept was not found. However, single technology bricks could be identified, which provide useful scientific insight for future aircraft configurations and the design of module-integrated ventilation concepts.

6 Closing remark

Author contributions T.D. and D.S. wrote the main manuscript text. All authors designed the measurement set-up and defined the research methodology. T.D. and P.L. performed all measurements, evaluated the data and prepared the figures. D.S. and I.G. supervised the evaluation and interpretation of the results. All authors reviewed the manuscript.

Data availability Selected data can be provided by the authors upon request.

Declarations

Conflict of interest The authors declare no competing interests.

References

1. IATA-International Air Transport Association, (2009) A global approach to reducing aviation emmisions. First stop: carbon-neutral growth from 2020, Montreal, Canada

2. Martinez I (2014) Aircraft Environmental Control, P.U.o. Madrid, Madrid, Spain

3. Schmidt, M., Müller, D., Gores, I., Markwart, M.: Numerical study of different air distribution systems for aircraft cabins. Technical University of Denmark, Denmark (2008)

4. Zhang, Z., Chen, X., Mazumdar, S., Zhang, T., Chen, Q.: Experimental and numerical investigation of airflow and contaminant transport in an airliner cabin mock-up. Build. Environ. **44**(1), 85–94 (2009)

5. Zhang, T., Li, P., Zhao, Y., Wang, S.: Various air distribution modes on commercial airplanes. part 1: experimental measurements. HVACR Res. **19**(3), 268–282 (2013)

6. Zhang, T., Li, P., Zhao, Y., Wang, S.: Various air distribution modes on commercial airplanes—part 2: computional fluid dynamics modeling and validation. HVACR Res. **19**(5), 457–470 (2013)

7. Bosbach, J., Lange, S., Dehne, T., Lauenroth, G., Hesselbach, F., Allzeit, M.: Alternative ventilation concepts for aircraft cabins. CEAS Aeronaut. J. **4**, 301–313 (2013)

8. Bosbach, J., Heider, A., Dehne, T., Markwart, M., Gores, I., Bendfeldt, P.: Evaluation of cabin displacement ventilation under flight conditions, in 28th international congress of the aeronautical sciences ICAS2012. Brisbane, Australia (2012)

9. Dehne T, Bosbach J and Heider A, (2014) Comparison of surface temperatures and cooling rates for different ventilation concepts in an A320 aircraft cabin under flight conditions, in 13th SCANVAC international conference on air distribution in rooms and airplanes Sao Pauo Brazil

10. Müller, D., Schmidt, M., Müller, B.: Application of displacement ventilation systems for air flow distribution in aircraft cabins. AST, Hamburg, Germany (2011)

11. Yan, W., Zhang, Y., Sun, Y., Li, D.: Experimental and CFD study of unsteady airbone pollutant transport within aircraft cabin mock-up. Build. Environ. **44**(1), 34–43 (2009)

12. Lange, P., Dehne, T., Schmeling, D., Dannhauer, A., Gores, I.: Realistic flight conditions on ground: new research facility for cabin ventilation. CEAS Aeronaut. J. **13**(3), 719–738 (2022)

13. Lange P, Dehne T, Schmeling D, Dannhauer A and Gores I, (2022) Comparison of two ceiling-based ventilation strategies for twin-aisle aircraft cabins, 17th International Conference on indoor air quality and climate, indoor air 2022; Reprinted with friendly permission from ISIAQ, Kuopio, Finland

14. Schmeling, D., Volkmann, A.: On the experimental investigation of novel low-momentum ventilation concepts for cooling operation in a train compartment. Build. Environ. **182**, 107–116 (2020)

15. Bosbach, J., Lange, S., Dehne, T., Heine, G., Hesselbach, F., Allzeit, M.: Alternative ventilation concepts for aircraft cabins. CEAS Aeronaut. J. **4**, 301–313 (2013)

16. EN 13129:2016, Railways application; air conditioning for main line rolling stock, comfort parameters and type tests, European committee for standardization, Bruxelles, 2016

17. Nilsson H. O, (2004) Comfort Climate Evaluation with Thermal Manikin Methods and Computer Simulation Models, Sweden: Department of Civil and Architectural Engineering Royal Institute of Technology; Department of Technology and Built Environment University of Gävle

18. EN ISO 7730, 2005 Ergonomics of the thermal environment—analytical determination and interpretation of thermal comfort using calculation of the PMV and PPD indices and local thermal comfort criteria, European commitee for standardization, Bruxelles

19. Dehne, T., Lange, P., Schmeling, D., Gores, I.: Micro-Jet ventilation—a novel ventilation concept for long-range aircraft cabins, ventilation 2022: 13th International Industrial Ventilation Conference for Contaminant Control. Canada, Toronto (2022)

20. ASHRAE, "ASHRAE,: Handbook of Funsamentals", p. 2001. American Society of Heating, Refrigeration and Air Conditiong Engineers Inc, Atlanta (2001)